2024 IEEE/RSJ International Conference on Intelligent Robots and Systems (IROS)
October 14-18, 2024. Abu Dhabi, UAE

Mobility Performance Characterization of Transformable Nano Rover for Lunar Exploration

Masataku Sutoh[1], Daichi Hirano[1], Mariko Inazawa[1], Yuta Kawai[1], and Hirotaka Sawada[1]

***Abstract*— In January 2024, a Japanese lunar lander successfully touched down on the moon as part of the Smart Lander for Investigating Moon (SLIM) mission. Accompanying the SLIM on its journey were two small rovers named lunar excursion vehicles (LEV-1 and 2). LEV-2, a transformable nano rover, was particularly designed to capture images of the SLIM on the lunar surface. During the mission, LEV-2 successfully maneuvered and captured images of the lander. Understanding the mobility characteristics of LEV-2 was crucial for the success of this task. This study analyzed the mobility characteristics of LEV-2 through numerical simulation and traveling tests. In the numerical simulation, a dynamics model of LEV-2 was first developed. Subsequently, the motion behaviors of LEV-2 were analyzed by utilizing the discrete element method. Traveling tests were then conducted using the LEV-2 engineering model on various terrains covered with a lunar regolith simulant. The results of both the numerical simulations and experiments revealed consistent trends across different moving modes of LEV-2. Furthermore, the simulation results indicated no significant deterioration in the mobility performance of LEV-2 on the moon when compared to that on the Earth. Based on the characteristics predicted from the simulation and the quantitative data obtained from the experiments, it was concluded that LEV-2 is supposed to travel at least 15° slopes on the moon.**

I. INTRODUCTION

A. Background and objectives

Lunar exploration has gained considerable attention worldwide. Hitherto, various unmanned rovers have made significant advancements in lunar exploration. The Soviet Union's Lunokhod, the world's first unmanned rover, traveled over 10 km on the lunar surface through remote control. This was followed by Lunokhod 2 [1]. In the 2010s, China's Yutu and Yutu 2 unmanned rovers explored the moon, with Yutu 2 being the first to explore the far side of the moon [2]. India's Pragyan rover, mounted on the Chandrayaan-3, became the first to reach the southern polar region of the moon in 2023, where potential water resources may exist. Japan is planning to launch the LUPEX rover mission in the 2020s for further investigating these water resources [3].

We have been developing a transformable nano rover for lunar exploration (Fig. 1). Our rover is small and lightweight, with a mass of approximately 228 g, when compared to those of aforementioned rovers. Although the rover functions are limited, it is ideal for space missions with limited payload mass and volume. Two of our rovers have been successfully integrated on ispace's HAKUTO-R lander, which attempted to land on the moon in April 2023, and JAXA's SLIM, which successfully landed on the moon in January 2024. The rover installed on the SLIM is known as LEV-2 and will be referred to as such in this study.

Fig. 1. Photograph of the transformable nano rover called Lunar Excursion Vehicle 2 (LEV-2). Courtesy of JAXA/TOMY Company/Sony Group Corporation/Doshisha University.

During the SLIM mission, two small rovers, named lunar excursion vehicles (LEV-1 and 2) accompanied the lander on its journey. These rovers were stowed aboard the lander and traveled together to the moon. Upon arriving at the lunar surface, the two rovers were separated by a few meters above the surface and deployed on the moon. Subsequently, each rover began to autonomously traverse the lunar surface. LEV-1, with a mass of 2.1 kg, moved by hopping and possessed communication capabilities to transmit data directly to the Earth [4]. LEV-2 moved around the lander and captured images of the lander. The images and telemetry collected by LEV-2 were transmitted to LEV-1 through Bluetooth communication and then relayed back to the Earth. During the SLIM mission, LEV-1 and 2 successfully navigated the lunar surface and captured images of the lander. Notably, LEV-2 holds the distinction of being the world's smallest and lightest lunar rover to date.

For LEV-2 to autonomously traverse the lunar surface, the mobility characteristics of the rover must be understood clearly. In this study, the mobility characteristics of LEV-2 were evaluated through numerical simulations and traveling tests. The dynamics model of LEV-2 was first developed, and its motion behavior was analyzed using the discrete element

[1] M. Sutoh, D. Hirano, M. Inazawa, Y. Kawai, and H. Sawada are with Japan Aerospace Exploration Agency, 3-1-1 Yoshinodai , Chuo, Sagamihara, Kanagawa, 252-5210, Japan. sutoh.masataku@jaxa.jp, hirano.daichi@jaxa.jp, inazawa.mariko@jaxa.jp, kawai.yuta@jaxa.jp, sawada.hirotaka@jaxa.jp

method (DEM) in the numerical simulations. Furthermore, the engineering model (EM) tests were conducted on a slope covered with a lunar regolith simulant, enabling a quantitative evaluation of the mobility characteristics of LEV-2.

B. Related studies

Various studies have utilized the DEM as a numerical analysis technique for machine-terrain interactions. Nakashima et al. analyzed the impact of gravity on wheel motion behavior using 2D DEM [5]. Johnson et al. conducted a DEM-based driving analysis for the wheels of a Martian rover [6]. Additionally, Ozaki et al. conducted experiments on the behavior of granular materials in various reduced-gravity environments at the International Space Station. Their results were compared with those of DEM-based numerical analysis under similar conditions. The results demonstrated the effectiveness of the DEM for ground behavior in various gravity environments [7]. Consequently, numerical simulations were performed using the DEM to analyze the fundamental behavior of LEV-2 on the moon.

The motion behaviors of rovers in lunar and Martian gravity environments have been analyzed through various experiments. When designing a lunar roving vehicle (LRV) during the Apollo program, experiments were conducted using a vehicle with 1/6 the mass of the actual LRV to simulate lunar gravity (approximately 1/6 of Earth's gravity, hereinafter 1/6 G) conditions on the ground [8]. Similarly, experiments were conducted using a rover with a mass of 1/3 that of the actual Martian rover to simulate its behavior in a Martian gravity environment (approximately 1/3 of the Earth's gravity) [9]. Although these experiments can simulate the load of a vehicle/rover under lunar/Martian gravity, they do not account for the gravity acting on the ground (regolith).

To simulate the behaviors of a rover and ground in a reduced gravity environment, an experiment utilizing the parabolic flight of an aircraft was conducted. In this experiment, the aircraft ascended and descended repeatedly, and an arbitrary reduced-gravity environment was created inside the aircraft. The motion behaviors of various wheels were observed by running the wheels in a sand bin installed on the aircraft. Based on the experiments conducted in the aircraft, Kobayashi et al. reported that the mobility performance of rigid wheels decreased in a reduced-gravity environment [10]. Similarly, Niksirat et al. demonstrated that the traction of elastic wheels is reduced by approximately 5-10% in Martian gravity and by 20% in lunar gravity [11]. Furthermore, Wong proposed a ground test method based on a mathematical model derived based on the data obtained from the aircraft experiments. In this method, the same mass model as that of an actual vehicle was utilized rather than a reduced mass model corresponding to the load under extraterrestrial gravity [12].

The mass and size of LEV-2 were extremely small when compared to the wheels in the aforementioned studies [10], [11]. Therefore, the applicability of the trends obtained from the existing studies to LEV-2 remains unclear. This study presents an experimental analysis of the mobility characteristics of LEV-2 by utilizing the same mass model as proposed by Wong [12], in addition to DEM-based analysis.

Fig. 2. Photograph of LEV-2s in the folded and transformed shapes. Courtesy of the JAXA/TOMY Company/Sony Group Corporation/Doshisha University.

The remainder of this paper is organized as follows. Section 2 presents an overview of LEV-2. Sections 3 and 4 discuss the numerical analysis based on the DEM and traveling tests conducted in the lunar regolith simulant, respectively. Lastly, Section 5 concludes the paper.

II. Transformable nano rover (LEV-2)

The overview and specifications of our transformable nano rover LEV-2 are presented in Fig. 2 and Table I, respectively. As shown on the left side of the figure, LEV-2 is spherical in the stowed condition; however, once deployed on the moon, it transforms into a running mode, as shown on the right side. LEV-2 primarily comprises a head, body, wheels, and stabilizer. The electronic devices installed on the body and head are listed in Table II, with each device undergoing environmental tests (considering various conditions, such as temperature and vibration) to ensure effectiveness during the SLIM mission. The structure and onboard equipment of the LEV-2 are reported in detail in [13].

LEV-2 autonomously navigates the lunar surface using a navigation algorithm installed in the onboard controller [14]. After deployment, the rover transitions from the stowed to the running mode and captures images of the surrounding environment using its rear camera. Subsequently, it moves forward away from the SLIM by processing the captured images onboard. Once a sufficient distance is reached, LEV-2 travels around the lander, continuously capturing images using its front camera. LEV-2 has a limited operational time of approximately 2 h on the moon if it operates under

TABLE I
SPECIFICATIONS OF LEV-2

Size	(folded) L 78 mm × W 90mm × H 78 mm
	(transformed) L 136 mm × W 123 mm × H 90 mm
Mass	approximately of 228 g
Wheel	⌀ 78 mm × W 40 mm

extreme conditions, such as temperatures as low as -20°C in the worst case scenario. Efficiency is crucial to maximizing the rover capabilities within this timeframe.

To facilitate autonomous travel, LEV-2 utilizes two wheels and a stabilizer. The stabilizer enables forward movement and turning without rotating the body. The wheel rotation centers are offset from the wheel centers by 12 mm to enhance the mobility performance. Each wheel of the LEV-2 is powered by two DC motors mounted within its body. These motors are connected to the wheels through a planetary gear system with a reduction ratio of 256:1, producing a no-load speed of 270°/s and a maximum continuous torque of 109 mNm. The motors are controlled by a PWM signal generated by the controller. LEV-2 can operate in two modes: the butterfly mode, where the left and right wheels rotate with no phase difference, and the crawl mode, where the wheels rotate with a phase difference. Additionally, when transitioning from the stowed mode to deployment, these motors are utilized to release latches on the wheel rotation axes.

III. Mobility behavior analysis of LEV-2 based on DEM

For LEV-2 to achieve autonomous driving on the lunar surface, it is imperative to have a thorough understanding of its basic mobility characteristics. We analyzed the motion behavior of LEV-2 in a lunar gravity environment using the DEM. This section outlines the DEM-based numerical analysis model that was utilized and presents the results of our analysis.

A. Coupled analysis model based on DEM

As shown in Fig. 3, the Altair Engineering Motion Solve and EDEM were utilized to analyze the mobility characteristics of LEV-2 on the lunar surface. Through the dynamic analysis software (Motion Solve), a mechanical model of LEV-2 was developed based on its actual dimensions and mass. This model comprised a main body section as well as left and right wheels. The head, body, and stabilizer of LEV-2 were modeled as single units in the main body section. The electronics and harnesses were simplified, and a dummy mass representing these components was placed at the center of gravity of the main body. The connection between the main body and the left and right wheels was modeled using rotation joints, enabling the simulation of the LEV-2 model by rotating the joints.

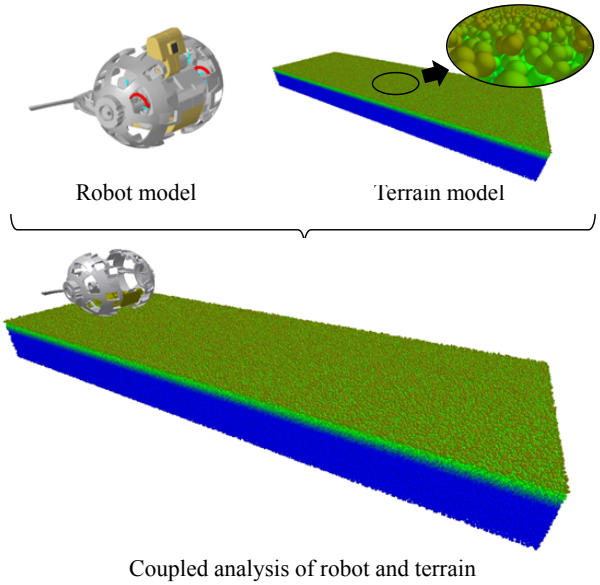

Fig. 3. Numerical analysis based on DEM.

The terrain was modeled as a collection of particles based on the DEM. The EDEM software can simulate the macroscopic behavior of a target terrain by setting various particle parameters, such as shape and friction behavior. A tri-sphere particle model was utilized to simulate the characteristics of the heterogeneous regolith. The Hertz-Mindlin model was utilized to define the interactions between the particles themselves and between the particles and the machine (LEV-2 main body and wheels). The terrain parameters for the particle model were roughly tuned to align with the quantitative data of traveling tests conducted using a lunar regolith simulant, as examined in Section 4. The parameters used are listed in Table III.

A coupled analysis of the mechanical model of LEV-2 developed in Motion Solve and the terrain constructed in EDEM were employed to analyze the behavior of LEV-2 in various gravity environments. During the simulation, the environmental acceleration can be adjusted, enabling the motion analysis of LEV-2 in different gravity environments. The process of this coupled analysis is outlined below.

TABLE II
ELECTRICAL COMPONENTS INSTALLED ON LEV-2.

Item	Number
Onboard controller (SONY SPRESENSE^{TM})	1
Camera	2 (Front and rear)
Bluetooth module	1
Inertial measurement unit	2
Motor	2
Motor driver	1
Rotary encoder	2
Battery	2
Micro switch	2

TABLE III
TERRAIN PARAMETERS FOR THE PARTICLE MODEL USED IN THE DEM. TO REDUCE COMPUTATIONAL COSTS, PARTICLE SIZE WAS SET LARGER THAN IN REALITY, AND ITS DISTRIBUTION WAS MODELED AS UNIFORM.

Properties	
Particle shape	tri-sphere
Sphere radius	1 mm
Particle density	2.8 g/cm^3
Coefficient of restitution	0.7
Coefficient of static friction	0.3
Coefficient of rolling friction	0.1

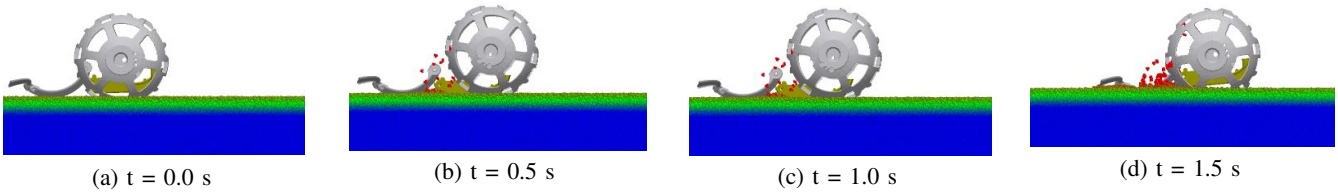

(a) t = 0.0 s (b) t = 0.5 s (c) t = 1.0 s (d) t = 1.5 s

(A) Flat terrain; butterfly mode.

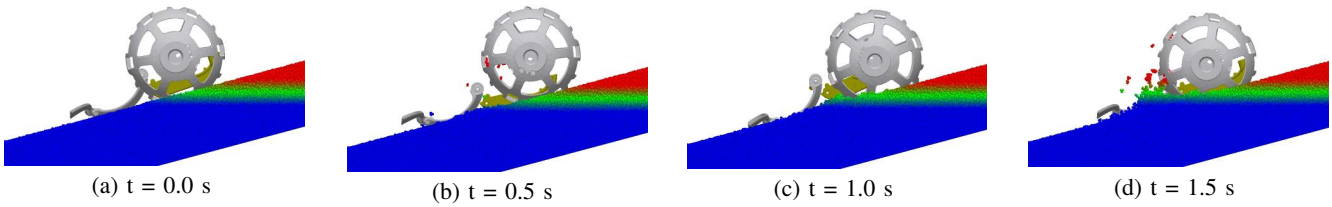

(a) t = 0.0 s (b) t = 0.5 s (c) t = 1.0 s (d) t = 1.5 s

(B) Sloped terrain with an angle of 15°; butterfly mode.

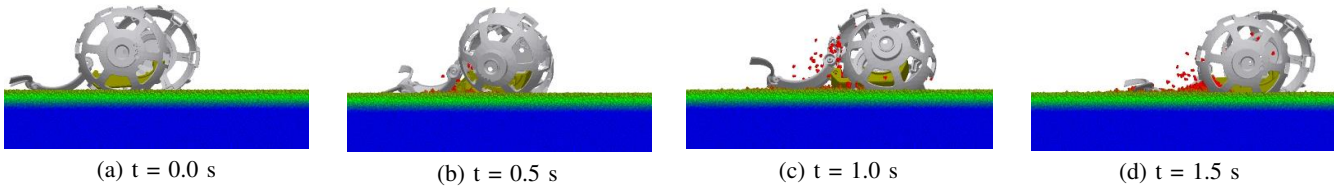

(a) t = 0.0 s (b) t = 0.5 s (c) t = 1.0 s (d) t = 1.5 s

(C) Flat terrain; crawl mode.

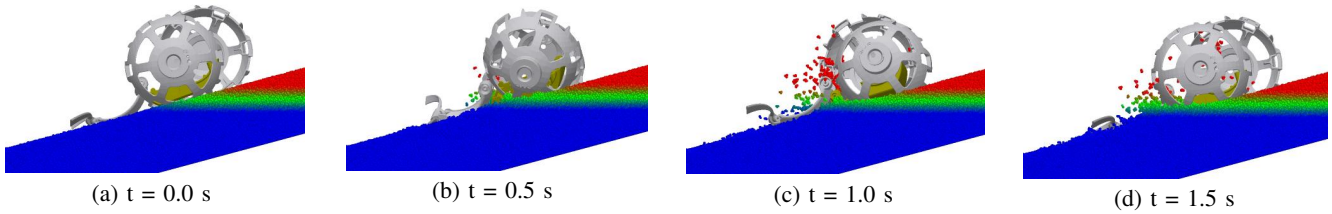

(a) t = 0.0 s (b) t = 0.5 s (c) t = 1.0 s (d) t = 1.5 s

(D) Sloped terrain with an angle of 15°; crawl mode.

Fig. 4. Images of simulation analyses on flat and sloped terrains in 1/6G environment. In the simulation, the wheels were rotated by the PWM control with a duty ratio of 80 % to mirror the actual motion of LEV-2. The colors of the parcles in the sandbox changes from blue, green to red according to their height.

1) The wheels of LEV-2 are rotated in Motion Solve.
2) The movement and deformation of particles caused by the driving wheels are calculated using EDEM.
3) The reaction force between the particles and LEV-2 caused by particle movement and deformation is returned to Motion Solve.
4) Motion Solve estimates the motion of LEV-2 and returns the result to EDEM.
5) Return to 2).

This iterative process is repeated every 1 ms for the specified simulation time to analyze the behavior of LEV-2 in the target terrain.

B. Simulation condition

As shown in Fig. 3, the simulation was performed in a sandbox with dimensions of 0.6 × 0.2 × 0.05 m. The sandbox was filled with 0.32 million particles, each comprising tri-sphere particles. The sandbox was tilted from 0° to 15° in increments of 5° to observe the behavior of LEV-2 moving on a slope. During the simulations, LEV-2 was initially placed on the ground surface with the ground prepared; after LEV-2 came to a stop, the left and right wheels of LEV-2 began to rotate. According to the motor characteristics of LEV-2, the wheels were rotated through PWM control with a duty ratio of 80%. Furthermore, simulations were conducted in the butterfly modes (phase difference: 0°) and crawl (phase difference: 180°) by altering the initial phase of the left and right wheels. Moreover, to analyze the effect of lunar gravity on the behavior of LEV-2, simulations were conducted under two gravity patterns of 1/6 and 1 G. The movement and wheel rotation of the LEV-2 were recorded at a frequency of 20 Hz.

C. Simulation results

The time series of LEV-2 simulated on 0° and 15° slope under 1/6 G is depicted in Fig. 4. On the flat terrain, LEV-2

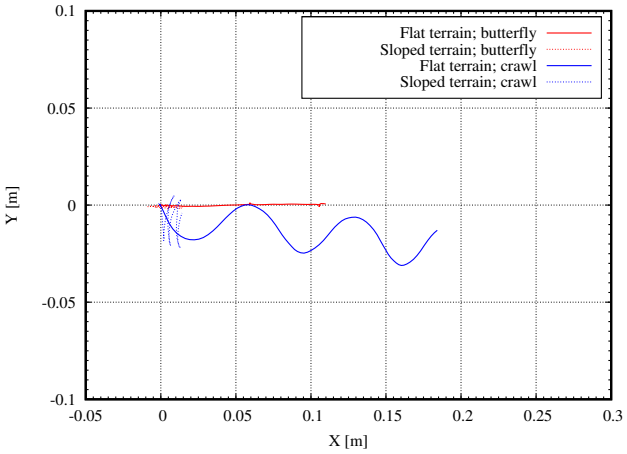

(a) X-Y plane

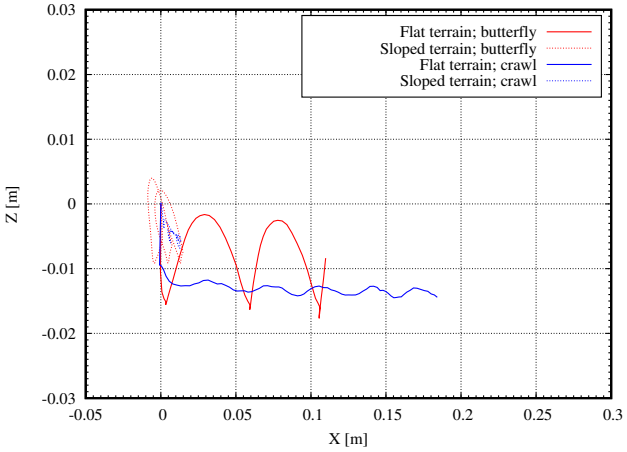

(b) X-Z plane

Fig. 5. Motion trajectory of LEV-2 based on numerical simulations. The results obtained from the flat and sloped terrains with an angle of 15° in 1/6G environment are illustrated. The X and Z axes indicate the horizontal and vertical directions, respectively.

smoothly moved forward as the wheels rotated in both the butterfly and crawl modes, as shown in Figs. 4(A) and (C). Meanwhile, LEV-2 managed to move forward on the slopped terrain, as shown in Figs. 4(B) and (D).

The trajectory of LEV-2 on 0° and 15° slope terrains under 1/6 G is shown in Fig. 5. In the butterfly mode (represented by the red line in the figure), LEV-2 exhibited minimal lateral movement, as observed in the X-Y plane trajectory in Fig. 5(a). A significant vertical attitude change could be observed in the trajectory of the X-Z plane, as shown in Fig. 5(b). Conversely, in the crawl mode (represented by the blue line in the figure), LEV-2 moved forward with minimal vertical attitude change while traversing from side to side. Similar trends were observed on the flat (solid line in the figure) and sloped terrains (dashed line in the figure).

The distances covered by LEV-2 at various slopes obtained under 1/6 G and 1 G are depicted in Fig. 6. The distance covered was calculated as that per wheel revolution. When LEV-2 moves across the terrain, its wheels may experience slippage, resulting in variations in the distance covered under

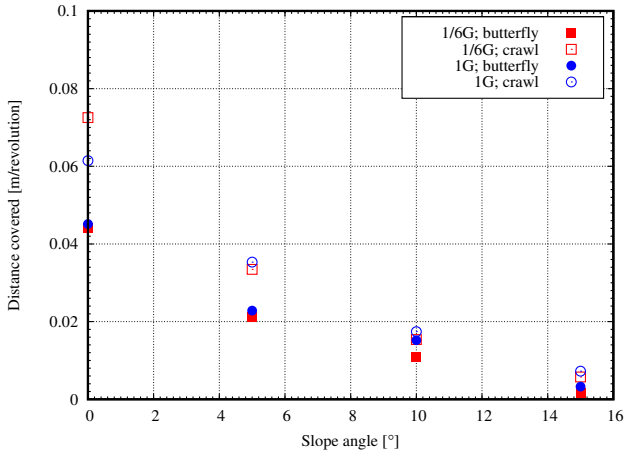

Fig. 6. Slope angle versus distance covered. The simulation results for the distance covered per wheel revolution are plotted.

different conditions. From the figure, the crawl mode (points unfilled in the figure) generally covered a greater distance when compared to the butterfly mode (points filled in the figure) for each scenario.

In both the butterfly and crawl modes shown in Fig. 6, the distance covered in each gravity scenario was almost identical in most cases. On the flat terrain, the distance covered in the crawl mode was even longer in 1/6 G scenario (unfilled square in the figure) than in the full gravity scenario (1G) (unfilled circles in the figure). As shown in Fig. 4, the wheels rolled over particles during movement. The effect of particle roll-up by the wheels was more pronounced in 1/6 G than in 1 G (see also the attached movie). Consequently, it was expected that the slippage of the wheel would increase in the 1/6 G scenario; however, it was observed that this effect on the slippage was negligible because the friction between the wheels and the ground significantly contributes to the slippage and was not significantly influenced by gravity.

IV. Slope Traveling Test in the Simulated Lunar Regolith

In addition to the numerical simulation earlier mentioned, traveling tests were conducted using the LEV-2 EM to quantitatively evaluate the mobility characteristics of LEV-2. This section provides an overview of the LEV-2 EM, the slope traveling test setup utilized, and presents the experimental conditions and results.

A. LEV-2 Engineering model

Based on the method proposed by Wong [12], we quantitatively estimated the mobility characteristics of LEV-2 from experiments using a similar mass model. An overview of the LEV-2 EM utilized in the experiment is shown in Fig. 7. This EM mirrors the size and mass of the LEV-2 flight model (FM) and possesses similar functions related to traveling, imaging, and communication. The FM operates autonomously without external commands. For the experiment, the software of the EM was modified to enable operation by the operator sending commands through Bluetooth from

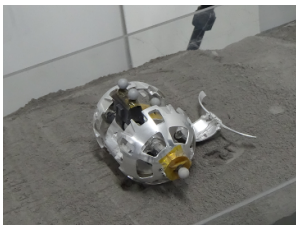

(a) Butterfly mode

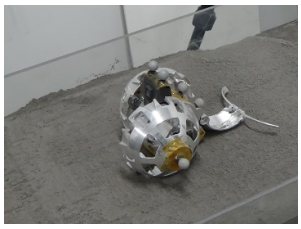

(b) Crawl mode

Fig. 7. Photograph of the LEV-2 EM for the traveling test, markers were attached to the LEV-2 EM.

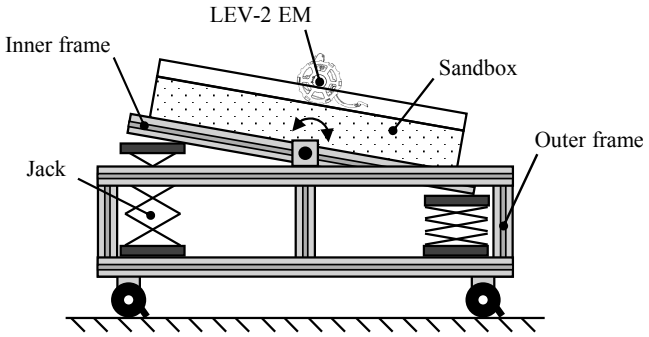

Fig. 8. Conceptual diagram of slope traveling test setup.

a control laptop. Although the LEV-2 FM utilized primary batteries, rechargeable batteries (lithium polymer, 3.7 V 400 mAh) were employed for the EM to facilitate repeated experiments. Infrared markers were affixed to the EM's surface during the experiment to measure the degree of movement.

B. Slope traveling test setup

A conceptual diagram of the slope traveling test setup is shown in Fig. 8. The test setup comprised outer and inner frame sections. Cylindrical shafts were attached to the middle of the inner frame section, directed by bearings fixed to the outer frame section. Two jacks were positioned at the front and back sides of the inner frame bottom. By adjusting the height of the jacks, the sandbox affixed to the inner frame section could be tilted at various angles. The dimensions of the sandbox were 0.5 $\times$ 0.3 $\times$ 0.2 m, filled with a lunar regolith simulant (Shimizu Corp.; FJS-1) [15] to a depth of 0.15 m.

Six 3D measurement cameras (Optitrack; PrimeX 13 W) were positioned on tripods around the slope traveling test setup. By integrating the images captured by these cameras with a software (Optitrack; Motive:Tracker) on a laptop, the movement of the LEV-2 could be measured with an accuracy within a few millimeters. Throughout the experiments, the movement of the LEV-2 was recorded at a frequency of 100 Hz using the system.

C. Experimental conditions

Traveling tests of the LEV-2 were conducted on various inclined terrains utilizing the slope traveling test setup. An overview of the traveling tests utilizing the LEV-2 is presented in Fig. 9. During the experiment, the regolith

Fig. 9. Photograph of the LEV-2 EM in the slope traveling test. LEV-2 traveled in the crawl mode over a sloped terrain.

simulant in the sandbox was initially loosened using a shovel and subsequently leveled to flatten its surface using a leveler. The shear strength of the terrain surface was measured using a shear vane tester, with values ranging from 0.5 to 0.8 cNm, corresponding to a minimum bulk density for the simulant.

After preparing the ground according to the aforementioned procedure, the LEV-2 was positioned on the ground surface. Control commands were then transmitted to the LEV-2, initiating its movement. The left and right motors of the LEV-2 were controlled through PWM with a duty ratio of 80%, and the wheels were rotated five times each on the flat and sloped terrains. Experiments were conducted in the butterfly and crawl modes by adjusting the initial phase of the wheel at the start of the experiment. The slope of the terrain was set to four patterns of 5° increments from 0° to 15°, with each condition being tested thrice to ensure reproducibility.

D. Experimental results and discussion

The trajectories of LEV-2 at slopes of 0° and 15° are shown in Fig. 10. This is a similar trend to the numerical simulation described in Section 3. In the butterfly mode, the left-right movement of the LEV-2 body was relatively limited, and vertical changes in attitude were observed. Conversely, when operating in the crawl mode, the LEV-2 body exhibited lateral movement while advancing with minimal vertical displacement.

The distance covered by the LEV-2 on terrain with different slope angles is shown in Fig. 11, along with the corresponding simulation results. The distance covered represents the distance per wheel revolution calculated from the total distance measured and number of wheel revolutions. Each data point reflects the average of three trials, with error bars denoting the range of values. Although the distance covered was greater in the crawl mode than in the butterfly mode in the simulation outlined in Section 3, this trend was not so pronounced from the experimental results. Based on this

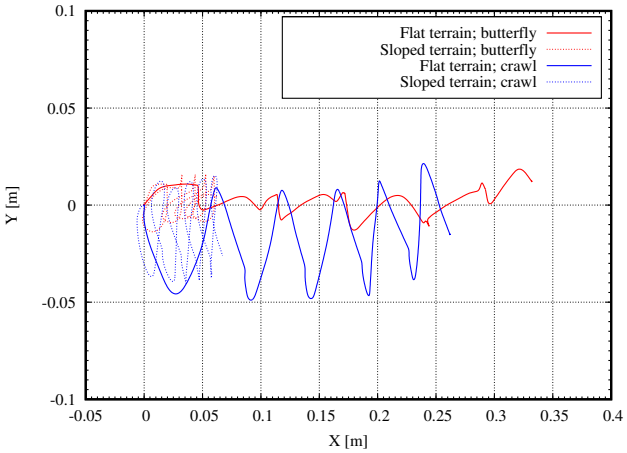

(a) X-Y plane

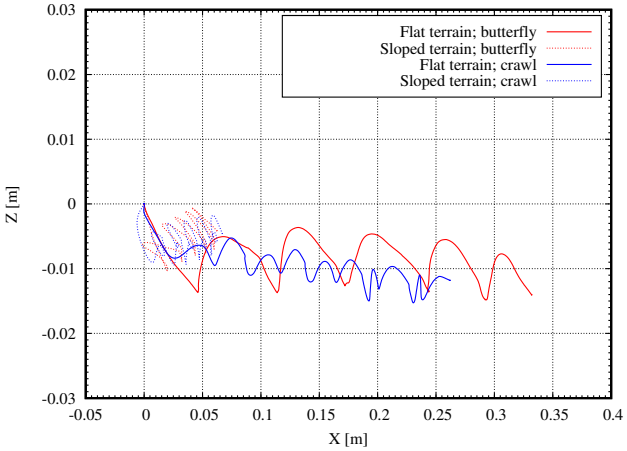

(b) X-Z plane

Fig. 10. Motion trajectory of LEV-2 obtained from the slope traveling tests. The results obtained from flat and sloped terrains with an angle of 15° are plotted.

observation, the flight software of LEV-2 was developed to allow LEV-2 to travel without actively adjusting the wheel phase difference.

From Fig. 11, it is seen that LEV-2 could travel over slopes of up to 15° in both simulation and experiments. This trend was also true in the simulation conducted in 1/6G, as shown in Fig. 6. This observation suggests that LEV-2 can travel at least 15° slopes on the moon.

When comparing the distance covered per wheel revolution of LEV-2 in Fig. 11, the distances estimated in the simulation slightly varied from those measured in the experiments. In this study, the focus of the numerical simulation was to understand the fundamental behavior of LEV-2, rather than fine-tuning the terrain parameters to fit with the experimental observation. Adjusting these parameters to concur with the experimental results may allow for a more accurate reproduction of the mobility characteristics of LEV-2.

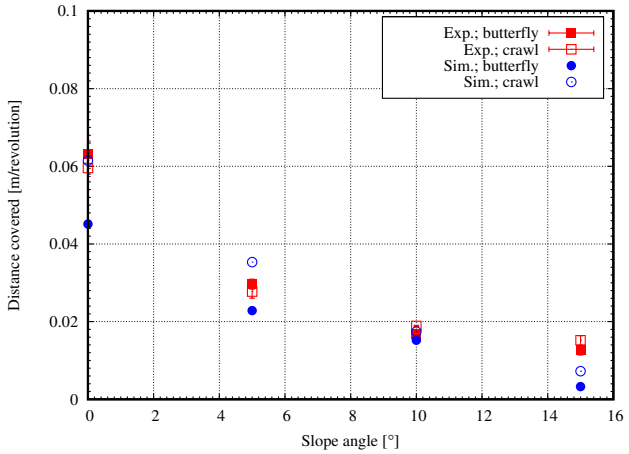

Fig. 11. Slope angle versus distance covered. The experimental results for the distance covered per wheel revolution are plotted along with the simulation results.

V. CONCLUSIONS

In this study, we analyzed the mobility characteristics of the transformable nano rover (LEV-2) through numerical simulations and traveling tests. Initially, a dynamics model was developed for the numerical simulation, and the motion behaviors were analyzed using DEM. Subsequently, a traveling test was conducted using the LEV-2 EM on various terrains covered with a lunar regolith simulant. The experiments aimed to quantitatively evaluate the mobility characteristics of LEV-2.

The numerical simulations and experimental results revealed similar trends for the two types of moving modes of LEV-2. Furthermore, although it has been suggested in the literature that the mobility performance of a wheel is reduced on the moon when compared to that on Earth, no significant performance deterioration was observed in the case of LEV-2, which has extremely small mass and size. Consequently, it was concluded that LEV-2 is supposed to travel at least 15° slopes on the moon.

As of August 2024, data on the motion behavior of LEV-2 on the moon are still under analysis. Future studies involve validating the trends obtained from numerical simulations by comparing the data obtained on the moon with those obtained from ground-based experiments. Furthermore, the terrain parameters of the numerical simulation will be adjusted to match the data obtained on the moon, enhancing the accuracy of the simulation. Simulations that can accurately predict the motion of a machine moving on the moon will contribute to the design and operation of various rovers in the future.

ACKNOWLEDGMENT

The authors would like to thank Y. Yoneda at TOMY Company, Ltd. and K. Watanabe at Doshisha University for their assistance with the hardware design and mechanism of the LEV-2. Further, we are grateful to M. Nagata and G. Sakoda at the SONY Group Corporation for the control software of LEV-2, particularly for the capturing and processing image and motor driving.

REFERENCES

[1] M. Malenkov, "Self-propelled automatic chassis of Lunokhod-1: History of creation in episodes," *Frontiers of Mechanical Engineering*, vol. 11, no. 1, pp. 60–86, 2016.

[2] L. Ding, R. Zhou, Y. Yuan, H. Yang, J. Li, T. Yu, C. Liu, J. Wang, S. Li, H. Gao, *et al.*, "A 2-year locomotive exploration and scientific investigation of the lunar farside by the Yutu-2 rover," *Science Robotics*, vol. 7, no. 62, p. eabj6660, 2022.

[3] T. Hoshino, S. Wakabayashi, M. Ohtake, Y. Karouji, T. Hayashi, H. Morimoto, H. Shiraishi, T. Shimada, T. Hashimoto, H. Inoue, *et al.*, "Lunar polar exploration mission for water prospection-JAXA's current status of joint study with ISRO," *Acta Astronaut.*, vol. 176, pp. 52–58, 2020.

[4] T. Yoshimitsu, "Small hopping robot for lunar exploration," in *Proc. 74th Int. Astronautical Congr. (IAC)*, Azerbaijan, 2023, pp. IAC–23–A3.2B.13.

[5] H. Nakashima and T. Kobayashi, "Effects of gravity on rigid rover wheel sinkage and motion resistance assessed using two-dimensional discrete element method," *J. Terramech.*, vol. 53, pp. 37–45, 2014.

[6] J. B. Johnson, A. V. Kulchitsky, P. Duvoy, K. Iagnemma, C. Senatore, R. E. Arvidson, and J. Moore, "Discrete element method simulations of Mars Exploration rover wheel performance," *J. Terramech.*, vol. 62, pp. 31–40, 2015.

[7] S. Ozaki, G. Ishigami, M. Otsuki, H. Miyamoto, K. Wada, Y. Watanabe, T. Nishino, H. Kojima, K. Soda, Y. Nakao, *et al.*, "Granular flow experiment using artificial gravity generator at International Space Station," *npj Microgravity*, vol. 9, no. 1, p. 61, 2023.

[8] F. Northon, "Engineer design test of mobility test article model GM–1," *US Army Test & Evaluation Command. NASA CR–102477*, 1967.

[9] M. Heverly, J. Matthews, J. Lin, D. Fuller, M. Maimone, J. Biesiadecki, and J. Leichty, "Traverse performance characterization for the Mars Science Laboratory rover," *J. Field Robotics*, vol. 30, no. 6, pp. 835–846, 2013.

[10] T. Kobayashi, Y. Fujiwara, J. Yamakawa, N. Yasufuku, and K. Omine, "Mobility performance of a rigid wheel in low gravity environments," *J. Terramech.*, vol. 47, no. 4, pp. 261–274, 2010.

[11] P. Niksirat, A. Daca, and K. Skonieczny, "The effects of reduced-gravity on planetary rover mobility," *Int. J. Robotics Research*, vol. 39, no. 7, pp. 797–811, 2020.

[12] J. Y. Wong, "Predicting the performances of rigid rover wheels on extraterrestrial surfaces based on test results obtained on earth," *J. Terramech.*, vol. 49, no. 1, pp. 49–61, 2012.

[13] D. Hirano, M. Inazawa, M. Sutoh, H. Sawada, Y. Kawai, M. Nagata, G. Sakoda, Y. Yoneda, and K. Watanabe, "Transformable nano rover for space exploration," *IEEE Robotics and Automation Lett.*, vol. 9, no. 4, pp. 3139–3146, 2024.

[14] M. Inazawa, D. Hirano, M. Sutoh, H. Sawada, M. Nagata, and G. Sakoda, "Autonomous control of Lunar Excursion Vehicle 2 (LEV-2)," in *Proc. Int. Conf. on Space Robotics 2024*, Luxembourg, 2024, p. TueS10T2.2.

[15] H. Kanamori, S. Udagawa, T. Yoshida, S. Matsumoto, and K. Takagi, "Properties of lunar soil simulant manufactured in Japan," in *Space 98*, 1998, pp. 462–468.